doi:10.1016/j.jmb.2011.09.044 J. Mol. Biol. (2011) 414, 699–712

Contents lists available at www.sciencedirect.com

Journal of Molecular Biology

journal homepage: http://ees.elsevier.com.jmb

Neuroprotective and Nootropic Drug Noopept Rescues α-Synuclein Amyloid Cytotoxicity

Xueen Jia[1]†, Anna L. Gharibyan[1]†, Anders Öhman[2], Yonggang Liu[1,3], Anders Olofsson[1] and Ludmilla A. Morozova-Roche[1]*

[1]*Department of Medical Biochemistry and Biophysics, Umeå University, SE-90187 Umeå, Sweden*
[2]*Department of Chemistry, Umeå University, SE-90187 Umeå, Sweden*
[3]*Department of Histology and Embryology, Chongqing Medical University, Chongqing, People's Republic of China*

Received 17 June 2011;
received in revised form
19 September 2011;
accepted 24 September 2011
Available online
1 October 2011

Edited by S. Radford

Keywords:
α-synuclein;
noopept;
amyloid;
cytotoxicity;
Parkinson's disease

Parkinson's disease is a common neurodegenerative disorder characterized by α-synuclein (α-Syn)-containing Lewy body formation and selective loss of dopaminergic neurons in the substantia nigra. We have demonstrated the modulating effect of noopept, a novel proline-containing dipeptide drug with nootropic and neuroprotective properties, on α-Syn oligomerization and fibrillation by using thioflavin T fluorescence, far-UV CD, and atomic force microscopy techniques. Noopept does not bind to a sterically specific site in the α-Syn molecule as revealed by heteronuclear two-dimensional NMR analysis, but due to hydrophobic interactions with toxic amyloid oligomers, it prompts their rapid sequestration into larger fibrillar amyloid aggregates. Consequently, this process rescues the cytotoxic effect of amyloid oligomers on neuroblastoma SH-SY5Y cells as demonstrated by using cell viability assays and fluorescent staining of apoptotic and necrotic cells and by assessing the level of intracellular oxidative stress. The mitigating effect of noopept against amyloid oligomeric cytotoxicity may offer additional benefits to the already well-established therapeutic functions of this new pharmaceutical.

Introduction

Parkinson's disease (PD) is the second most common progressive neurodegenerative disorder characterized by resting tremor, bradykinesia, and cognitive and emotional disorders among other cardinal signs. The incidence increases with increasing age and 1–2% of the population above the age of 65 develop PD. The pathological characteristics of PD include the formation of intraneuronal fibrillar inclusions such as Lewy bodies, composed primarily of α-synuclein (α-Syn), and the preferential loss of dopaminergic neurons in the substantia nigra.[1–4] α-Syn aggregation is an invariant feature of both sporadic and familial forms of PD and has been observed in the pathogenesis of multiple system atrophy and dementia with Lewy bodies as well. These and other neurodegenerative disorders characterized by α-Syn inclusions are collectively known as synucleinopathies.[5] Strong genetic, physiological, and biochemical evidence support the central role of α-Syn in the pathogenesis of PD:[6–10] specifically, three mutations in α-Syn (A30P, A53T, and E46K) as well as duplication/triplication in a region encompassing the α-Syn gene are sufficient to cause early-onset familial PD; wild-type and mutants of α-Syn form amyloids under a variety of *in vitro* conditions,

*Corresponding author. E-mail address: Ludmilla.Morozova-Roche@medchem.umu.se.

† X.J. and A.L.G. contributed equally to this work.

Abbreviations used: AFM, atomic force microscopy; HSQC, heteronuclear single quantum correlation; LDH, lactate dehydrogenase; PD, Parkinson's disease; ROS, reactive oxygen species; ThT, thioflavin T; WST-1, water-soluble tetrazolium salt; α-Syn, α-synuclein.

and all familial PD mutations accelerate the aggregation of α-Syn *in vitro*.[7,11–14] α-Syn is a 14-kDa soluble, intrinsically unfolded protein,[5,15] which is expressed in all neurons and enriched at many synaptic terminals.[16] Because it is intrinsically disordered, α-Syn is a highly adjustable protein; its conformation depends drastically on the environment and it can easily self-assemble into amyloid oligomers and fibrils under various conditions.[9,10,12,13] Among multiple amyloid forms of α-Syn, small soluble oligomers and protofibrils populated on-pathway to amyloid fibrils are viewed as the most neurotoxic species in both intra- and extracellular toxicity.[5,17] This implies that the formation of insoluble amyloid fibrils may serve as a protective pathway sequestrating toxic species from the cellular environment,[18,19] consistent with the presence of Lewy bodies in surviving neurons.

The dopaminergic neuronal loss and easing of clinical symptoms for a period by administering L-dopa suggest that there is a link between α-Syn aggregation and dopamine metabolism. Several studies demonstrated that L-dopa, dopamine, its oxidative intermediates, and other catechols can modulate α-Syn aggregation by inducing the formation of soluble oligomeric intermediates that are resistant to SDS, not interacting with thioflavin T (ThT), and stabilized from conversion into amyloid fibrils.[20–24] Experimental evidence that amyloid formation pathways can be effectively manipulated by other small molecules has been accumulated as well;[25] for example, the oligomeric cytotoxicity can be alleviated by curcumin, which also reduces reactive oxygen species (ROS) levels and protects cells against apoptosis;[26] epigallocatechin gallate remodels and detoxifies both cellular and *in vitro* produced α-Syn aggregates,[27] while methylene blue, belonging to the phenothiazine class of compounds, selectively inhibits amyloid oligomerization but promotes fiber formation in a dose-dependent manner.[28]

Here, we studied the mitigating effect of the novel neuroprotective and nootropic (cognitive enhancer) drug noopept (Noopept®) on the pathological consequences of α-Syn amyloid formation. Noopept (*N*-phenylacetyl-L-prolylglycine ethyl ester) is a water-soluble proline-containing synthetic dipeptide as presented in Fig. 1, showing that this is not a planar molecule with both N and C termini modified with phenol ring and ethyl ester, respectively. It was selected from the series of acyl-proline-containing dipeptides due to its distinct neuroprotective properties.[29] The drug action is based on its antioxidant and anti-inflammatory effects, its inhibitory activity towards the neurotoxicity of excess of calcium and glutamate, and its ability to improve blood rheology.[30,31] We have shown recently that noopept improves spatial memory and increases

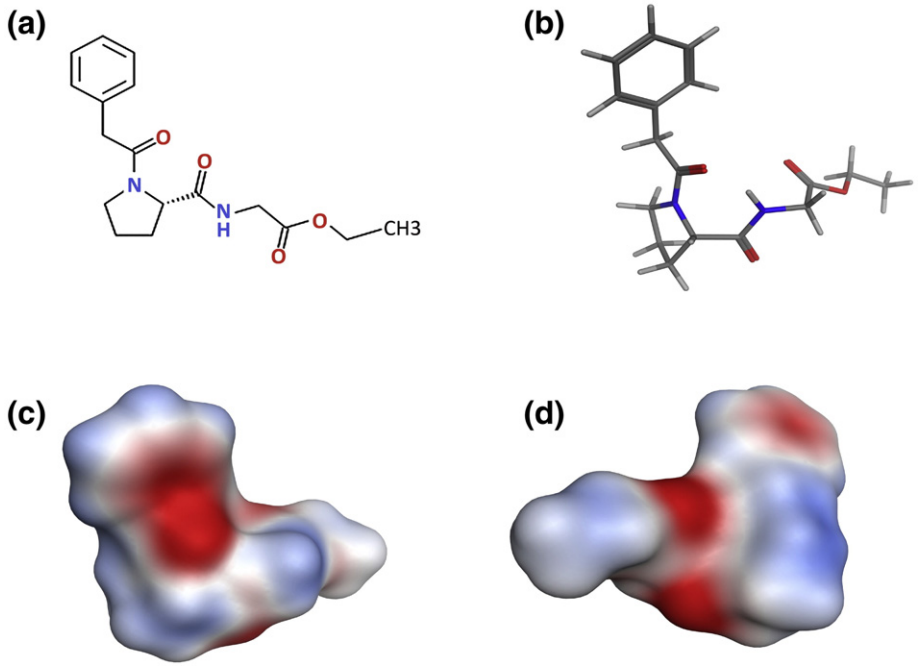

Fig. 1. Structure of noopept. (a) Chemical formula of noopept. (b) The three-dimensional model of noopept in a stick representation, as well as its electrostatic surface from the same view as the stick model (c) and rotated by 180° (d). Red and blue represent negative and positive electrostatic surface potentials, respectively.

immunoreactivity to Aβ amyloid in an Alzheimer's disease mice model following olfactory bulbectomy operation.[32] Noopept has a wide safety margin, and its pharmacokinetics indicate specific bioavailability for the brain. In essence, noopept is between 200 and 50,000 times more potent than piracetam as a nootropic agent on a dose-for-dose basis.[33] Noopept produces positive nootropic and cognitive effect in animal models at 0.01 to 0.8 mg/kg concentrations.[32,34,35] Currently, noopept tablets are used for treating cognitive deficiency of cerebrovascular and posttraumatic origin and recommended in dosages from 10 to 30 mg/day‡.

By using spectroscopic techniques, NMR, atomic force microscopy (AFM), and cellular assays, we demonstrated the modulating effect of noopept on the α-Syn amyloid formation pathways and its rescuing neuroblastoma SH-SY5Y cells from amyloid-induced cytotoxicity, which adds a significant value to its established neuroprotective pharmacological properties.

Results

NMR spectroscopy of α-Syn titrated with noopept

The effect of noopept on the α-Syn structure was monitored by recording heteronuclear two-dimensional [^{1}H–^{15}N]-HSQC (heteronuclear single quantum correlation) spectra of α-Syn at an α-Syn:noopept molar ratio of 1:0, 1:0.5, 1:1, 1:2, 1:5, 1:10, 1:20, and 1:50. We did not observe significant chemical shift and peak intensity changes, not even when the spectra of α-Syn alone and with the highest concentration of noopept were compared. Figure 2 summarizes these results, showing representative values at an α-Syn:noopept molar ratio of 1:20; all chemical shift changes were below 0.003, and peak intensity ratios for all resonances were ca 1.0. Therefore, it is unlikely that noopept binds specifically to monomeric α-Syn, which is not surprising given that α-Syn is a natively unfolded molecule and does not possess a sterically specific binding site.

Effect of noopept on the kinetics of α-Syn amyloid formation

The effect of noopept on the kinetics of α-Syn amyloid formation was monitored by the ThT binding assay (Fig. 3), as the specific interactions of this dye with the cross-β-sheet-containing amyloids lead to a rise in fluorescence emission. In the absence of noopept, the time dependence of amyloid formation of α-Syn in 10 mM sodium phosphate, pH 7.4, at 37 °C was characterized by a 1-day lag phase, during which ThT fluorescence remained unchanged; this was followed by a growth phase, when fluorescence intensity increased, reaching a plateau level after ca 5 days. In the presence of 1:1 and 1:10 molar ratios of α-Syn to noopept, the aggregation proceeded much faster. In both cases, the lag phase was almost eliminated, the growth phase was much steeper, especially at the higher concentration of noopept, and the plateau was reached after 2 days and 1 day, respectively (Fig. 3). Therefore, noopept clearly shifts the α-Syn self-assembly process towards fibrillization.

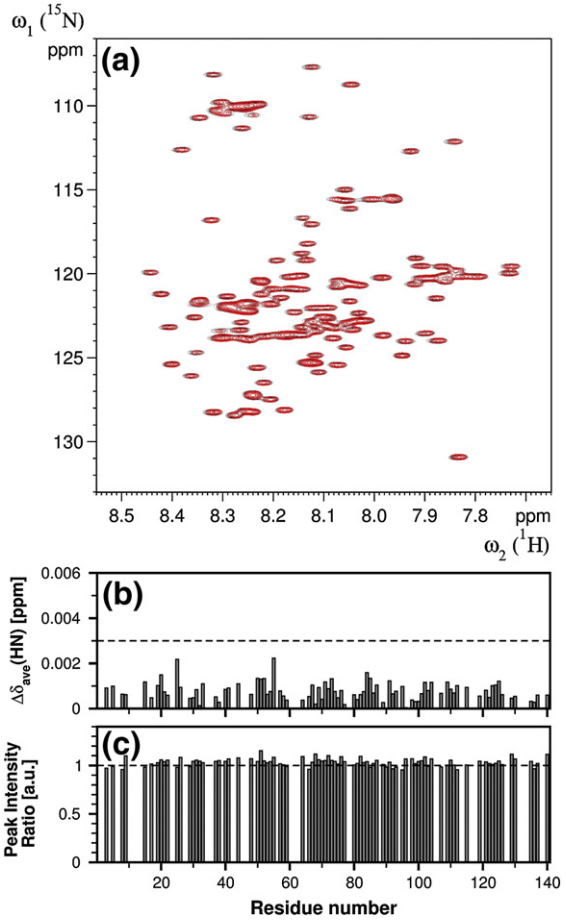

Fig. 2. Effect of noopept on α-Syn monitored by NMR spectroscopy. (a) The amide resonances in [^{1}H–^{15}N]-HSQC experiments recorded on 50 μM α-Syn in the absence (black contour levels) or presence of noopept (1:20 molar ratio, red contour levels) are nearly identical, with only minor (b) chemical shift and (c) intensity changes observed. For clarity, the [^{1}H–^{15}N]-HSQC experiment recorded in the presence of noopept is drawn at higher contour levels. The horizontal line drawn at $\Delta\delta_{ave} = 0.003$ (a) represents a cutoff level for significant chemical shift changes.

‡ http://noopept.com

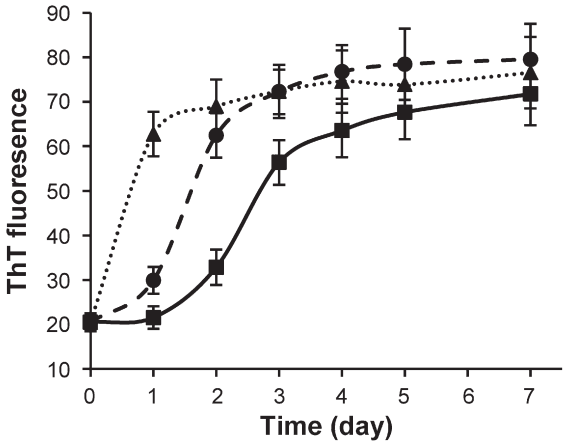

Fig. 3. Noopept promotes α-Syn fibrillation. Time dependence of α-Syn amyloid formation monitored by ThT fluorescence: α-Syn was aged alone (continuous line denoted by squares) and at 1:1 (broken line with circles) and 1:10 (dotted line with triangles) molar ratios of α-Syn and noopept.

Effect of noopept on α-Syn β-sheet-dependent aggregation

Changes in the secondary structure during incubation of α-Syn under amyloid-forming conditions in the presence and absence of noopept were monitored by far-UV CD (Fig. 4a–c). Freshly dissolved α-Syn was characterized by a typical random-coil CD spectrum with a major negative peak centered at 198 nm (Fig. 4a). During the first day of incubation in the absence of noopept, there were no changes in α-Syn CD spectra reflecting the lag phase of amyloid formation (Fig. 4d). The shift towards a β-sheet-like spectrum became evident during the growth phase, and after 5 days of incubation, the far-UV CD spectrum of α-Syn displayed a characteristic β-sheet pattern with a major minimum observed at ca 218–220 nm and a maximum centered at ca 200–205 nm (Fig. 4a). Some increase in the spectral maximum and minimum amplitudes was observed upon further incubation up to 7 days, yet the spectral shape did not change. In the presence of a 1:1 molar ratio of noopept to α-Syn, the rapid development of β-sheet CD spectrum was observed on the second day of incubation, and subsequent changes reflected only a small ellipticity increase in the positive band centered at 200–205 nm, while the ellipticity at the 218- to 220-nm minimum effectively reached a plateau (Fig. 4b and d). When noopept was added to α-Syn at a 10-fold excess, the lag phase was completely abolished and α-Syn acquired a β-sheet conformation within ca 1 day of incubation (i.e., the signals at both the 205-nm maximum and the 220-nm minimum plateaued and displayed only a small increase upon further incubation). These results correlate well with the α-Syn kinetics of amyloid formation observed by ThT fluorescence binding assay (Fig. 3), indicating that noopept shifts the self-assembly process towards the formation of cross-β-sheet-rich amyloid fibrils.

AFM imaging of α-Syn amyloids

The process of α-Syn amyloid self-assembly was monitored by AFM imaging as shown in Fig. 5. Freshly dissolved α-Syn in the absence of noopept was amyloid-free, and after 1 day of incubation, only particles with a height of ca 0.4–0.7 nm, as measured in the AFM cross-sections, were observed, which, according to their dimensions, most likely corresponded to monomeric and tetrameric species[36] (Fig. 5a). After 3 days of incubation corresponding to the growth phase (Figs. 3b and 4d), a few thin fibrils with a height of ca 2.0 nm and with a length of up to 1 μm and even longer were spontaneously assembled (Fig. 5b), but enlarged round-shaped oligomers with a height of ca 1.0–2.0 nm remained as the dominant species; their dimensions indicate that these oligomers are from octamers to ecosinomers.[36,37] After 7 days of incubation, the quantity of fibrils increased, which were significantly thicker and up to 5–6 nm in height in the AFM cross-sections, but a micrometer in length or shorter (Fig. 5c, c1). At the same time, round-shaped aggregates with a height of ca 2.0–3.0 nm were also significantly populated; their AFM dimensions suggest that they are ecosinomers and larger oligomers (Fig. 5c, c1).

In the presence of a 1:1 ratio of α-Syn to noopept, some oligomeric species that were of ca 1.5 to 2.0 nm height in the AFM cross-sections as well as thin, short protofibrils that were of ca 3.0 nm height and ≤100 nm length were formed after 1 day of incubation (Fig. 5d). After 3 days, fibrils that were up to 5 μm long and with a 7.0–9.0 nm in height were developed (Fig. 5e). Upon further incubation for up to 7 days, the fibrils grew even longer, exceeding 5 μm and intertwined with each other, forming ca 15-nm-thick bundles as shown in the representative AFM cross-section in Fig. 5f (f1).

The α-Syn co-incubated with a 10-fold excess of noopept undergone very rapid amyloid formation. Within 1 day, a large amount of fibrils (a few micrometers long and up to 12 nm in height in the AFM cross-sections) were observed (Fig. 5g); their quantity increased progressively with further incubation, and after 7 days, clumps of thick amyloid fibrils of up to ca 15 nm height in AFM cross-sections were populated (Fig. 5i, i1). It is interesting to note that similar to the α-Syn fibrils in the absence of noopept, the fibrils formed in the presence of 10-fold excess of noopept also tended to break into shorter stretches upon prolonged incubation from 3 to 7 days, that is, from ca 5 μm length and longer (Fig. 5h) to 1–2 μm and shorter (Fig. 5i). Therefore, the AFM

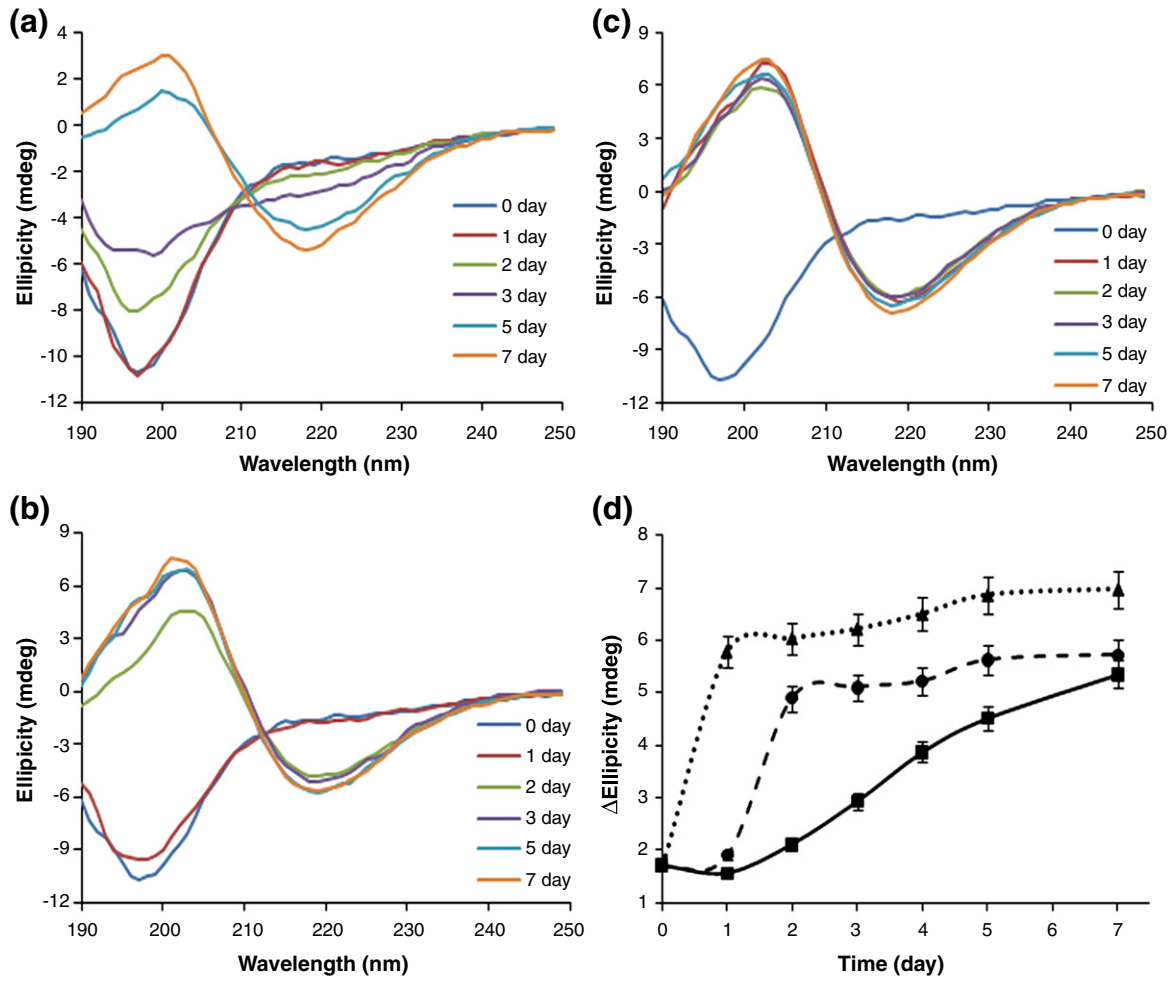

Fig. 4. Effect of noopept on α-Syn amyloid formation monitored by far-UV CD. Far-UV CD spectra of α-Syn alone (a) and at 1:1 (b) and 1:10 (c) molar ratios of α-Syn and noopept; the age of the samples is shown in captions. Time dependence of changes in ellipticity at 218 nm (d); the samples are marked as in Fig. 1b.

imaging of the amyloid assemblies (fibril formation *versus* oligomers) is consistent with the kinetics of amyloid formation followed by the spectroscopic techniques as presented above (Figs. 3 and 4).

Noopept rescues cytotoxicity induced by α-Syn amyloids in SH-SY5Y cells

The viability of SH-SY5Y neuroblastoma cells in the presence of α-Syn amyloids and noopept was assessed by the water-soluble tetrazolium salt (WST-1) assay (Fig. 6). In viable cells, WST-1 undergoes reduction by mitochondrial dehydrogenases (succinate–tetrazolium reductase system) to soluble formazan, which serves as an indicator of the amount of metabolically active cells. SH-SY5Y cells were treated with 50 μM aged α-Syn amyloids for 24 h and 48 h. Freshly dissolved α-Syn added at the same concentration did not affect the cell viability after both 24 h and 48 h of co-incubation; that is, the latter was characterized by higher error bars, indicating that changes were not significant. When cells were treated with 1-day-aged α-Syn species, the viability did not change after 24 h of co-incubation and reduced by ca 20% after 48 h. The cell viability was reduced by ca 20% after 24 h and by ca 50% after 48 h when 3- and 7-day-aged α-Syn amyloids were added. However, when SH-SY5Y cells were treated with α-Syn amyloids in the presence of either 1:1 or 1:10 molar ratios of α-Syn to noopept, cell survival was completely restored to the level of untreated cells after 24 h of co-incubation and to ca 90% after 48 h, respectively. Noopept itself did not affect the cell viability (Fig. 6) as well as the amyloid incubation buffer when added to cells (data not shown).

The effect of α-Syn amyloids on SH-SY5Y cell viability was also assessed by monitoring lactate dehydrogenase (LDH) release (Fig. 7a), which showed good agreement with the WST-1 assay results. LDH is a cytosolic enzyme that is rapidly released into the cell culture supernatant upon

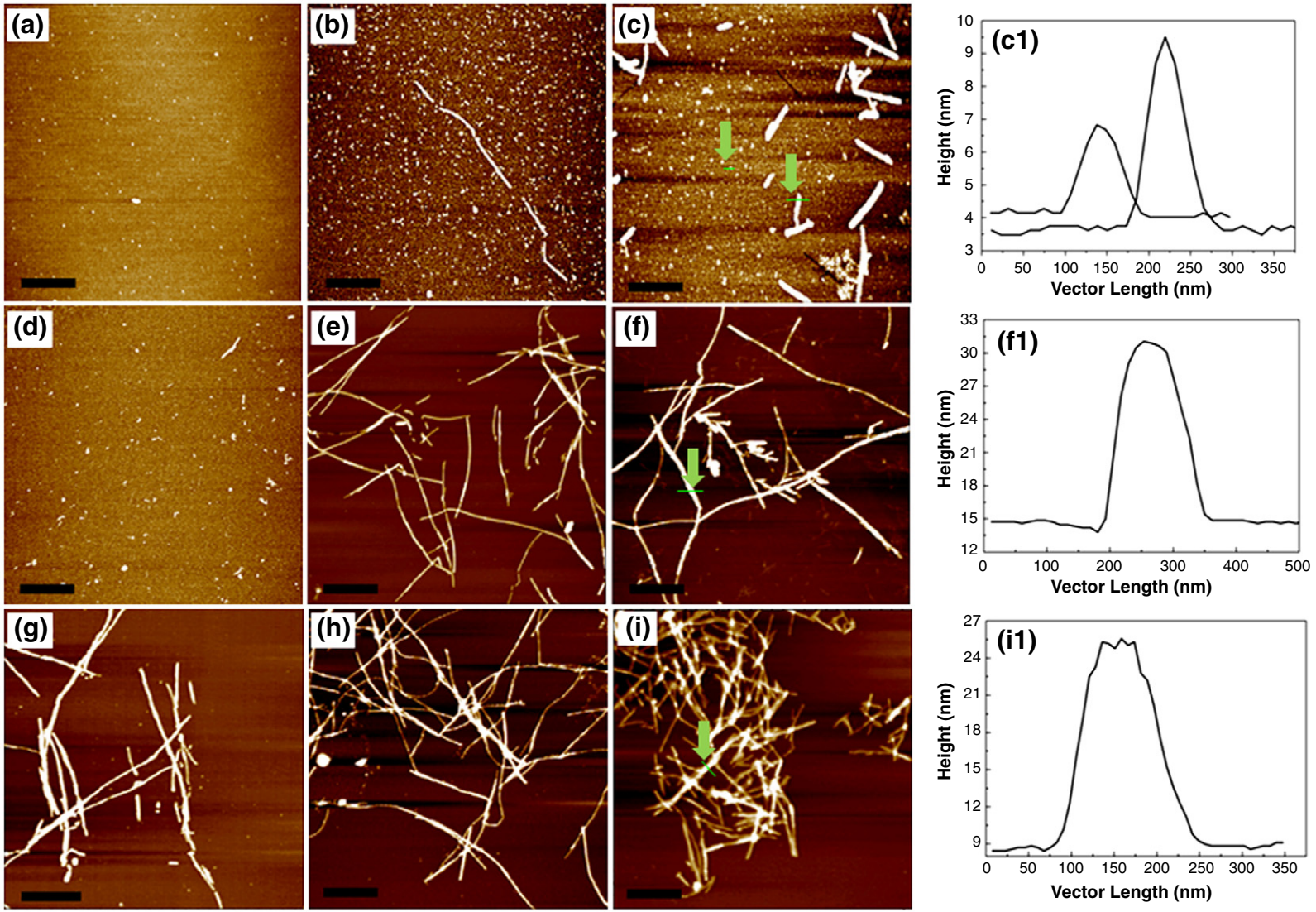

Fig. 5. AFM images of α-Syn amyloids. AFM images of α-Syn alone incubated for 1 day (a), 3 days (b), and 7 days (c); samples containing 1:1 and 1:10 molar ratios of α-Syn and noopept co-incubated for 1 day (d and g), 3 days (e and h), and 7 days (f and i). In all images, the *xy*-scale is 5 μm × 5 μm. Representative cross-sections of amyloid structures; the place of cross-sections in the original images is shown by a green line and arrows (c1 corresponds to c; f1 to f; and i1 to i).

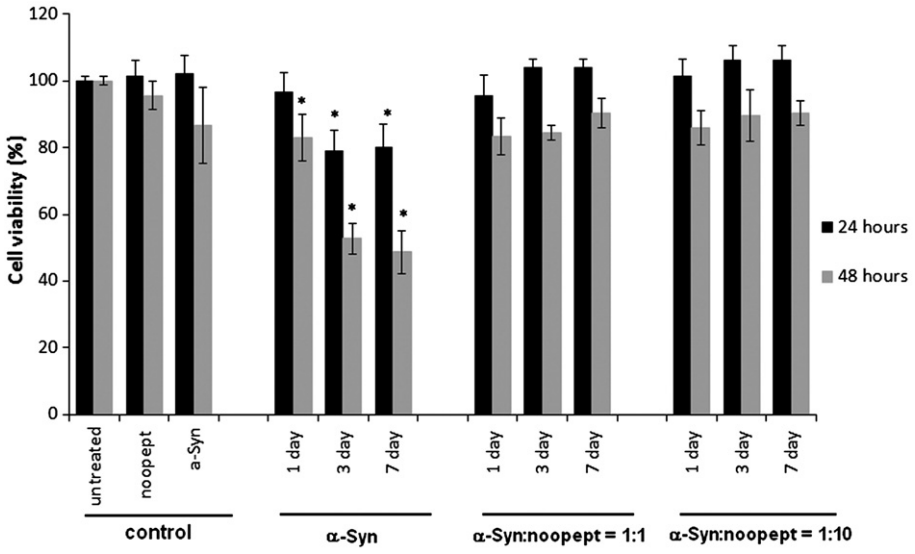

Fig. 6. Noopept rescues α-Syn amyloid induced cytotoxicity on SH-SY5Y cells as measured by the WST-1 assay. The percentage of viable cells is shown in the *y*-axis, and the samples added to cells are described along the *x*-axis. Cell viability was measured after 24 h (black bars) and 48 h (gray bars) of co-incubation with amyloids.

damage of the plasma membrane, serving as a measure of cell injury. The sample with 7-day-aged α-Syn amyloids caused a significant rise in LDH release, which was entirely abolished when the amyloid samples containing noopept either at 1:1 or 1:10 molar ratio of α-Syn to noopept were added to cells. In control measurements, freshly dissolved α-Syn, noopept alone, and the amyloid buffer did not affect LDH release. Thus, noopept rescues the cytotoxicity of α-Syn amyloids by inducing the sequestration of the toxic amyloid oligomers into less harmful fibrillar material.

Noopept decreases ROS level induced by α-Syn amyloids

ROS are by-products of normal cellular oxidative processes; however, their level rises significantly upon stress conditions induced by adding α-Syn amyloids (Fig. 7b and c). The ROS level increased significantly in SH-SY5Y cells upon addition of 7-day-aged α-Syn amyloids as monitored by fluorescence of dichlorofluorescein, which is an oxidized product of 2,7-dichlorofluorescein diacetate. The observations were performed by measuring the fluorescence intensity of stained cells in a 96-well plate (Fig. 7b) and under a fluorescent microscope (Fig. 7c, left, upper panel). The fluorescence decreased progressively when the samples contained increasing concentration of noopept, that is, 1:1 and 1:10 molar ratios of α-Syn to noopept (Fig. 7b and c, upper panel). Noopept itself, freshly dissolved α-Syn, and the amyloid buffer did not cause an increase in dichlorofluorescein fluorescence above the level of untreated cells within experimental error. As the production of ROS is likely induced by amyloid oligomers, their sequestration from solution under the influence of noopept effectively reduces the level of ROS.

Fluorescent staining of SH-SY5Y cells

Combined staining of SH-SY5Y cells with fluorescent-labeled Annexin V and propidium iodide was also performed to validate the effect of noopept on amyloid-induced cytotoxicity (Fig. 8). Annexin V is a protein that binds specifically to phosphatidylserine on the cell surface, when the latter is transferred from the inner to the outer leaflet of the cell membrane bilayer during early apoptosis, while propidium iodide penetrates through the damaged plasma membranes and stains DNA fragments during necrosis or late apoptosis. In control experiments, untreated cells as well as cells in the presence of noopept alone (500 μM) and freshly dissolved α-Syn did not display any staining, and the bright-field images acquired simultaneously confirmed that the cells were healthy. In the presence of 1- and 3-day-aged α-Syn amyloids, cells were stained with both dyes displaying green (Annexin V) and red (propidium iodide) fluorescence observed under a fluorescent microscope (Fig. 8). However, cells treated with 1-day-aged amyloids showed stronger staining with Annexin V, indicating predominantly apoptotic-type cell death, than cells in the presence of 3-day-aged amyloids, which displayed brighter red propidium iodide staining, suggesting an increasing contribution of necrotic-type death. Propidium

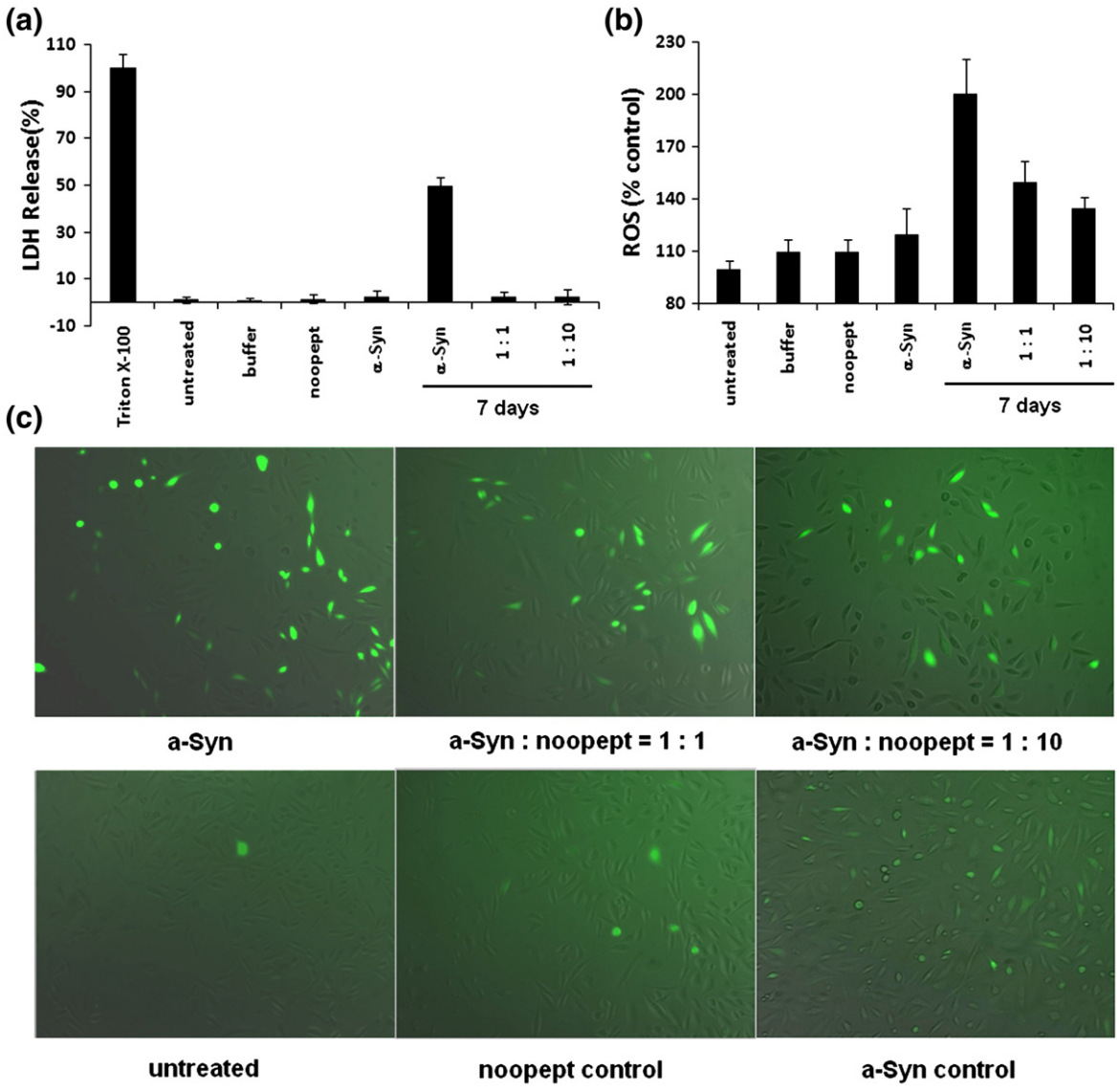

Fig. 7. Protective effect of noopept on SH-SY5Y cells treated with α-Syn amyloids by monitoring LDH release and ROS. (a) The percentage of LDH release after 6 h of co-incubation with the samples of interest is shown in the *y*-axis, and the samples added to cells are described along the *x*-axis. (b) ROS level in SH-SY5Y cells estimated by DCF fluorescence. The percentage of ROS proportional to DCF fluorescence in treated compared to untreated cells is shown on the *y*-axis, and the samples added to cells are described along the *x*-axis. (c) ROS level in SH-SY5Y cells monitored by DCF fluorescence via a fluorescence microscope with 10× magnification. Samples added to cells are denoted in captions.

iodide staining was dominant in the SH-SY5Y cell sample to which 7-day-aged amyloids were added, showing that the majority of cells die via necrotic pathways. Bright-field images of the samples treated with 1- and 3-day-aged α-Syn amyloids showed shrinking and compaction of some cells, characteristic of their apoptotic death, while cells to which 7-day-aged amyloids were added displayed rather necrotic morphology characterized by lysed cell membranes (Fig. 8).

Fig. 8. Morphology and Annexin V/propidium iodide staining of SH-SY5Y cells treated with α-Syn amyloids and noopept. Bright-field and fluorescent images (Annexin V, green fluorescence; propidium iodide, red fluorescence) were taken at the same time over the same area. Control samples with untreated cells, treated with noopept alone and with freshly dissolved α-Syn are shown in the upper panel as indicated in captions. Cells treated with 1, 3 and-7-day aged α-Syn amyloids with and without noopept are shown below as indicated in captions. All images are acquired with 20× magnification.

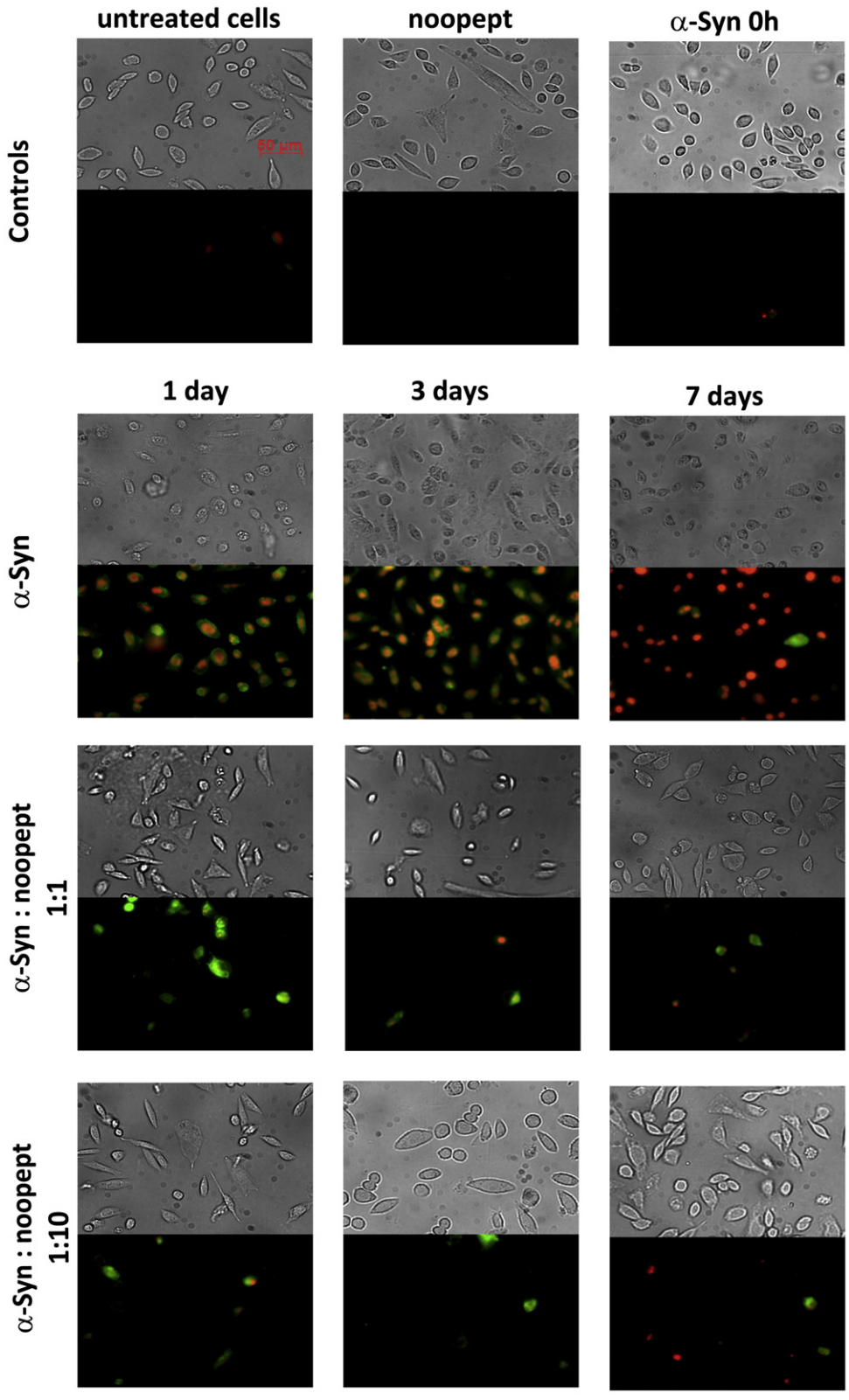

Fig. 8 (*legend on previous page*)

By contrast, upon addition to SH-SY5Y cells of amyloids together with noopept at 1:1 and 1:10 molar ratios of α-Syn to noopept, their propidium iodide fluorescent staining did not exceed the control level. The staining with Annexin V was observed only when 1-day-aged amyloids in the presence of equimolar ratio of noopept were added and the staining was reduced to the control level when the molar ratio of α-Syn to noopept increased to 1:10. In all noopept-containing samples, cells displayed predominantly healthy morphology in bright-field imaging (Fig. 8). Thus, the α-Syn amyloids produced in the presence of noopept display reduced cytotoxicity since noopept rescues from both apoptotic cell death caused by the amyloid oligomers by reducing their quantity in solution, and it also reduces the necrotic cell death caused by short fibrils by promoting fibrillar elongation (Figs. 5 and 8).

Discussion

The novel proline-containing dipeptide drug noopept was designed as an analog of piracetam, which belongs to the first generation of nootropic drugs.[38] Noopept, however, produces a nootropic effect at much lower concentrations and can be applied over a wider range of pathological conditions; for example, it also displays anxiolytic effects and is used in anxiety treatment.[39,40] It has been demonstrated that noopept affects synaptic transmission in central neurons,[41] decreases activity of stress-induced kinases, and increases expression of neutrophines in rat hippocampus;[42] it prevents oxidative damage and apoptosis in normal and Down's syndrome human cortical neurons as well.[30] Since many neurodegenerative conditions are accompanied by amyloid formation and amyloid cytotoxicity, we have shown here for the first time that noopept significantly modulates the amyloid assembly of α-Syn, the amyloidogenic protein involved in PD and other neurodegenerative synucleinopathies. There is another well-known example of epigallocatechin gallate compound that promotes conversion of toxic amyloid oligomers into nontoxic aggregates.[27,43] Here, we have also observed that aggregation might be beneficial for a model system in which aggregated α-Syn is given to cells as an exogenous species. As noopept is used as a drug, the further stringent evaluation of the *in vivo* conditions in animal and other models is required to insure the safety of drug usage, although, to date, the clinical administration of noopept gave only positive results without noticeable side effects.[39]

By using the ThT binding assay, far-UV CD spectroscopy, and AFM, we have demonstrated that in the presence of increasing concentrations of noopept, the lag phase in α-Syn amyloid assembly, where toxic oligomers are highly populated, practically disappeared (Figs. 3 and 4). At the same time, the overall fibrillation was promoted (Fig. 5), as reflected in enhanced ThT fluorescence and rapid development of typical β-sheet far-UV CD spectra. Moreover, if in the absence of noopept significant populations of amyloid oligomers were observed even after 7 days of incubation and fibrils were typically less than a micrometer in length (Fig. 5c), in the presence of 1:10 molar ratio of α-Syn to noopept, we already did not observe any oligomers after 1 day and the fibrils grew much longer, reaching a few micrometers, and three to four times thicker as measured in the AFM cross-sections (Fig. 5).

It is important to note that noopept does not bind to specific binding sites in monomeric α-Syn molecule; this is evident from [^{1}H–^{15}N]-HSQC spectra recorded in the absence and presence of noopept, showing a lack of significant chemical shift changes for the sequence-specifically assigned amide resonances of the α-Syn molecule (Fig. 2). Due to the presence of the phenol ring and proline group in its structure, noopept most likely exerts its fibrillation-promoting effect via nonspecific hydrophobic interactions with amyloid oligomers and fibrils. Given that noopept is a small molecule, its phenol ring can be readily available for the interactions with the phenol stacking if such takes place during the polypeptide amyloid assembly.[44] Indeed, α-Syn possesses a few Phe residues, which can potentially contribute to the π-stacking. It has been suggested and convincingly demonstrated using model peptide sequences that in addition to cross-β-sheet formation, the π-stacking of planar aromatic rings can also contribute to fibrillar self-assembly and stability.[44,45] Further high-resolution structural studies will reveal the precise mechanism of noopept interactions with α-Syn amyloids.

As the amyloid cytotoxicity is attributed primarily to oligomeric and protofibrillar species,[5,17,36,37] the enhanced fibrillation propensity can be beneficial, entrapping potentially harmful structures within less harmful mature amyloid fibrils and insoluble fibrillar clumps that effectively serve as a sink for toxic compounds. In the case of α-Syn, a wide range of oligomeric species displayed toxicity as evident from Figs. 5 to 8. Indeed, in the 1-day-aged sample, there were monomeric α-Syn present as specs in the AFM images with a height of 0.4 nm and larger oligomers with a height of 0.7 nm, which likely correspond to tetramers, as estimated from AFM cross-section analysis and calculation of particle volume by the spherical cap approximation.[34,40] The latter induced mostly apoptotic-type cell death as demonstrated by Annexin V and propidium iodide fluorescent staining and typical apoptotic cell morphology observed in the bright-field microscopy.[46] In the 3-day amyloid sample, the larger oligomers with a height of ca 1–2 nm were highly populated as evident in the

AFM imaging, corresponding to ecosinomers and even larger oligomers;[34,40] they were characterized by β-sheet structure as shown by ThT binding and far-UV CD, and these species were highly toxic, causing mixed apoptotic and necrotic cell deaths (Fig. 8). The 7-day-aged amyloid sample containing ecosinomers and larger oligomers (2–3 nm height) and short fibrils induced significant decreases in cell viability via a predominantly necrotic pathway (Fig. 8). Apart from toxic oligomers, necrotic cell death can also be induced by short fibrils as has been shown previously[47] and which were obviously present in this sample.

By contrast, the long mature fibrils of α-Syn formed in the presence of noopept were not toxic. This was corroborated by the restored viability of SH-SY5Y neuroblastoma cells monitored by WST-1 and LDH release assays (Figs. 6 and 7), lack of fluorescent staining with Annexin V and propidium iodide (Fig. 8), and reduction of oxidative stress (Fig. 7). While the major effect of noopept can be attributed to promoting fibrillation *versus* oligomerization (Figs. 3–5), its additional protective effect on cells *per se* in the presence of amyloids cannot be also excluded as this has been shown previously for hydrogen-peroxide-induced toxicity.[30]

In conclusion, noopept's ability to rescue amyloid cytotoxicity by redirecting harmful oligomeric and protofibrillar species into fibrillar aggregates and thus removing them from free floatation adds value to the other beneficial properties of this novel pharmaceutical compound and should be considered in therapeutic strategies targeting PD and other amyloid-related neurodegenerative disorders.

Materials and Methods

Materials

Wild-type and ^{15}N-labeled α-Syn were obtained from AlexoTech AB (Umeå, Sweden). Noopept (*N*-phenylacetyl-L-prolylglycine ethyl ester, MW 319) was designed and synthesized at the State V. V. Zakusov Institute of Pharmacology, Russian Academy of Medical Sciences (RAMS).[48] All other chemicals were purchased from Sigma (USA) unless stated differently. The amyloid samples were produced by incubation of 200 μM α-Syn in 10 mM sodium phosphate buffer, pH 7.4, at 37 °C under continuous gentle magnetic stirring.

Molecular modeling

A three-dimensional model of noopept was generated in the Molecular Operating Environment program, version 2009.10 (Chemical Computing Group Inc., Canada), by using simulated annealing followed by energy minimization (MMFF94x force field). The Molecular Operating Environment program was also used for preparing a stick image and electrostatic surface of noopept.

NMR spectroscopy

NMR experiments were carried out at 10 °C on a Bruker AVANCE spectrometer operating at 600 MHz (proton frequency) and equipped with a 5-mm triple-resonance, pulsed-field z-gradient cryoprobe. Heteronuclear two-dimensional [^{1}H–^{15}N]-HSQC spectra were recorded by using 50 μM α-Syn in 10 mM sodium phosphate buffer, pH 7.4, and 5% D_2O. Recorded experiments were processed using NMRPipe,[49] and peak positions and intensities were determined in NMRView.[50] The weighted average of the ^{1}H and ^{15}N chemical shift difference ($\Delta\delta_{ave} = (0.5[\Delta\delta(^{1}H)^2 + (0.2\Delta\delta\ (^{15}N))^2])1/2$) and the ratio of peak intensities between the different experiments were derived and presented by using the software Grace (plasma-gate.weizmann.ac.il/Grace), together with the previously reported ^{1}H and ^{15}N chemical shift assignment for α-Syn.[51,52]

ThT binding assay

ThT binding amyloid assay was carried out as described previously.[46] Fluorescence measurements were performed on a Jasco spectrofluorimeter FP 6500 (Jasco, Japan), using excitation at 440 nm, measuring emission between 460 and 520 nm, and taking intensity at 485 nm as a measure of ThT binding. Excitation and emission slits were set at 5 nm.

Circular dichroism

The far-UV CD spectra were recorded on a Jasco J720 CD UV spectrometer at room temperature, using a 1-mm light path quartz cell. Relative ellipticity is presented.

Atomic force microscopy

AFM measurements were performed on a PICO PLUS microscope (Agilent, USA) in a tapping mode using a 100-μm scanner with acoustically driven cantilevers operating at a resonance frequency in the 320- to 370-kHz range. Scanning resolution was 512×512 pixels. The scanning was performed in trace and retrace to avoid the scan artifacts. Specimens were diluted in Milli-Q water, incubated on freshly cleaved mica for 10 min, subsequently washed with 2×200 μl Milli-Q water, and dried overnight at room temperature. To determine the dimensions of amyloid species, we carried out a cross-section analysis of height images using PICO PLUS software.

Cell culture

SH-SY5Y cells were cultured in Dulbecco's modified Eagle's medium supplemented with 10% (v/v) fetal bovine serum and antibiotics in a 5% CO_2 humidified atmosphere at 37 °C. Cells were plated at a density of 10^4 cells/well in 96-well plates; after 24 h of incubation, the medium was changed before incubation with amyloid samples. Samples of α-Syn solutions were initially diluted in the culture medium and then added to the cells at a final concentration of 50 μM.

WST-1 cell viability assay

In order to evaluate cell viability, we added 10 μl of WST-1 reagent (Roche, Germany) per 100 μl of cell culture and we incubated samples at 37 °C for 4 h. Absorbance was measured by an ELISA plate reader (Sunrise, Tecan, USA) at 450 nm. Cell viability was expressed as a percentage of the absorbance in wells containing cells treated with amyloids compared to the control untreated cells.

LDH release

After the incubation of cells with α-Syn amyloids, 100 μl of culture medium was taken from the wells, mixed with 100 μl of LDH reaction solution (prepared according to the manufacturer's instructions, Roche), and incubated at room temperature for 30 min. Absorbance was measured at 492 nm using an ELISA plate reader. Untreated cells (low control) and those treated with 1% (v/v) Triton X-100 (high control) were used to determine spontaneous and maximum release of LDH, respectively. The percentage of cell cytotoxicity was calculated as:

$$\text{Cytotoxicity} = \frac{\text{experimental} - \text{low control}}{\text{high control} - \text{low control}} \times 100\%$$

Measurement of intracellular ROS formation

The formation of intracellular ROS was measured using a fluorescent probe, 2,7-dichlorofluorescein diacetate (Invitrogen, Sweden), as described in the literature.[53] After incubation of cells with α-Syn amyloids in a 96-well plate for 6 h, dichlorofluorescein diacetate (10 μM final concentration) was added to each well and the cells were incubated in dark conditions at 37 °C for 1 h. The fluorescence intensity of dichlorofluorescein (the oxidized species of dichlorofluorescein diacetate) was measured by a Jasco fluorescence spectrometer using excitation at 485 nm and emission at 535 nm. The fluorescence in untreated cells was taken as 100%. Specimens were also examined under an Axiovert 40 CFL fluorescent microscope (Carl Zeiss MicroImaging, Germany) with a 10× magnification.

Annexin V/propidium iodide staining

In order to stain cells with the Annexin V-FLUOS Staining Kit (Roche), containing Annexin V-fluorescein and propidium iodide, we cultured cells in 8-well BD Falcon culture slides (BD Biosciences, Sweden). After incubation with 50 μM α-Syn amyloids for 48 h, cells were washed with phosphate-buffered saline and covered with the Annexin V-FLUOS labeling solution prepared according to the manufacturer's instructions (Roche). The slides were incubated at room temperature for 15–20 min. Specimens were examined under an Axiovert 40 CFL fluorescent microscope (Carl Zeiss MicroImaging) equipped with an AxioCam MRm digital camera, with the use of an AxioVision image analyzing software.

Statistical analysis

All experiments were performed in triplicate or duplicate. Statistical analysis was performed by using Student's paired *t* test, and data are shown as mean ± SEM. $p < 0.05$ was considered significant.

Acknowledgements

We thank Professors Sergey B. Seredinin, Rita U. Ostrovskaya, and Tatyana A. Gudasheva (Institute of Pharmacology, RAMS, Moscow) as well as Dr. Marina A. Gruden (P. K. Anokhin Institute of Normal Physiology, RAMS, Moscow) for kindly providing noopept and for very fruitful discussions. This work was supported by the Swedish Medical Research Council, the Kempe Foundation, the Swedish Brain Foundation, the O. E. and Edla Johanssons Vetenskapliga Stiftelse, and the Umeå Insamlingsstiftelsen.

References

1. Simuni, T. & Hurtig, H. I. (2000). Parkinson's disease: the clinical picture. In *Neurodegenerative Dementias* (Clark, C. M. & Trojanowski, J. Q., eds), pp. 193–203, McGraw-Hill, New York, NY.
2. Gelb, D. J., Oliver, E. & Gilman, S. (1999). Diagnostic criteria for Parkinson disease. *Arch. Neurol.* **56**, 33–39.
3. Pakkenberg, B., Moller, A., Gundersen, H. J., Mouritzen Dam, A. & Pakkenberg, H. (1991). The absolute number of nerve cells in substantia nigra in normal subjects and in patients with Parkinson's disease estimated with an unbiased stereological method. *J. Neurol., Neurosurg. Psychiatry*, **54**, 30–33.
4. Damier, P., Hirsch, E. C., Agid, Y. & Graybiel, A. M. (1999). The substantia nigra of the human brain. II. Patterns of loss of dopamine-containing neurons in Parkinson's disease. *Brain*, **122**, 1437–1448.
5. Uversky, V. N. (2008). Alpha-synuclein misfolding and neurodegenerative diseases. *Curr. Protein Pept. Sci.* **9**, 507–540.
6. Kruger, R., Kuhn, W., Muller, T., Woitalla, D., Graeber, M., Kosel, S. *et al.* (1998). Ala30Pro mutation in the gene encoding alpha-synuclein in Parkinson's disease. *Nat. Genet.* **18**, 106–108.
7. Conway, K. A., Lee, S. J., Rochet, J. C., Ding, T. T., Williamson, R. E. & Lansbury, P. T., Jr (2000). Acceleration of oligomerization, not fibrillization, is a shared property of both alpha-synuclein mutations linked to early-onset Parkinson's disease: implications for pathogenesis and therapy. *Proc. Natl Acad. Sci. USA*, **97**, 571–576.
8. Singleton, A. B., Farrer, M., Johnson, J., Singleton, A., Hague, S., Kachergus, J. *et al.* (2003). Alpha-synuclein locus triplication causes Parkinson's disease. *Science*, **302**, 841.
9. Maraganore, D. M., Wilkes, K., Lesnick, T. G., Strain, K. J., de Andrade, M., Rocca, W. A. *et al.* (2004). A

limited role for DJ1 in Parkinson disease susceptibility. *Neurology*, **63**, 550–553.
10. Singleton, A., Gwinn-Hardy, K., Sharabi, Y., Li, S. T., Holmes, C., Dendi, R. *et al.* (2004). Association between cardiac denervation and parkinsonism caused by alpha-synuclein gene triplication. *Brain*, **127**, 768–772.
11. Conway, K. A., Harper, J. D. & Lansbury, P. T., Jr (2000). Fibrils formed in vitro from alpha-synuclein and two mutant forms linked to Parkinson's disease are typical amyloid. *Biochemistry*, **39**, 2552–2563.
12. Li, J., Uversky, V. N. & Fink, A. L. (2001). Effect of familial Parkinson's disease point mutations A30P and A53T on the structural properties, aggregation, and fibrillation of human alpha-synuclein. *Biochemistry*, **40**, 11604–11613.
13. Fredenburg, R. A., Rospigliosi, C., Meray, R. K., Kessler, J. C., Lashuel, H. A., Eliezer, D. & Lansbury, P. T., Jr. (2007). The impact of the E46K mutation on the properties of alpha-synuclein in its monomeric and oligomeric states. *Biochemistry*, **46**, 7107–7118.
14. Brown, D. R. (2010). Oligomeric alpha-synuclein and its role in neuronal death. *IUBMB Life*, **62**, 334–339.
15. Weinreb, P. H., Zhen, W., Poon, A. W., Conway, K. A. & Lansbury, P. T., Jr. (1996). NACP, a protein implicated in Alzheimer's disease and learning, is natively unfolded. *Biochemistry*, **35**, 13709–13715.
16. Totterdell, S., Hanger, D. & Meredith, G. E. (2004). The ultrastructural distribution of alpha-synuclein-like protein in normal mouse brain. *Brain Res.* **1004**, 61–72.
17. Walsh, D. M. & Selkoe, D. J. (2004). Oligomers on the brain: the emerging role of soluble protein aggregates in neurodegeneration. *Protein Pept. Lett.* **11**, 213–228.
18. Caughey, B. & Lansbury, P. T. (2003). Protofibrils, pores, fibrils, and neurodegeneration: separating the responsible protein aggregates from the innocent bystanders. *Annu. Rev. Neurosci.* **26**, 267–298.
19. Lambert, M. P., Barlow, A. K., Chromy, B. A., Edwards, C., Freed, R., Liosatos, M. *et al.* (1998). Diffusible, nonfibrillar ligands derived from Abeta1–42 are potent central nervous system neurotoxins. *Proc. Natl. Acad. Sci. USA*, **95**, 6448–6453.
20. Burke, W. J., Kumar, V. B., Pandey, N., Panneton, W. M., Gan, Q., Franko, M. W. *et al.* (2008). Aggregation of alpha-synuclein by DOPAL, the monoamine oxidase metabolite of dopamine. *Acta Neuropathol.* **115**, 193–203.
21. Rekas, A., Knott, R. B., Sokolova, A., Barnham, K. J., Perez, K. A., Masters, C. L. *et al.* (2010). The structure of dopamine induced alpha-synuclein oligomers. *Eur. Biophys. J.* **39**, 1407–1419.
22. Mazzulli, J. R., Mishizen, A. J., Giasson, B. I., Lynch, D. R., Thomas, S. A., Nakashima, A. *et al.* (2006). Cytosolic catechols inhibit alpha-synuclein aggregation and facilitate the formation of intracellular soluble oligomeric intermediates. *J. Neurosci.* **26**, 10068–10078.
23. Leong, S. L., Cappai, R., Barnham, K. J. & Pham, C. L. (2009). Modulation of alpha-synuclein aggregation by dopamine: a review. *Neurochem. Res.* **34**, 1838–1846.
24. Pham, C. L., Leong, S. L., Ali, F. E., Kenche, V. B., Hill, A. F., Gras, S. L. *et al.* (2009). Dopamine and the dopamine oxidation product 5,6-dihydroxylindole promote distinct on-pathway and off-pathway aggregation of alpha-synuclein in a pH-dependent manner. *J. Mol. Biol.* **387**, 771–785.
25. Yang, D. S., Yip, C. M., Huang, T. H., Chakrabartty, A. & Fraser, P. E. (1999). Manipulating the amyloid-beta aggregation pathway with chemical chaperones. *J. Biol. Chem.* **274**, 32970–32974.
26. Wang, M. S., Boddapati, S., Emadi, S. & Sierks, M. R. (2010). Curcumin reduces alpha-synuclein induced cytotoxicity in Parkinson's disease cell model. *BMC Neurosci.* **11**, 57.
27. Bieschke, J., Russ, J., Friedrich, R. P., Ehrnhoefer, D. E., Wobst, H., Neugebauer, K. & Wanker, E. E. (2010). EGCG remodels mature alpha-synuclein and amyloid-beta fibrils and reduces cellular toxicity. *Proc. Natl Acad. Sci. USA*, **107**, 7710–7715.
28. Necula, M., Breydo, L., Milton, S., Kayed, R., van der Veer, W. E., Tone, P. & Glabe, C. G. (2007). Methylene blue inhibits amyloid Abeta oligomerization by promoting fibrillization. *Biochemistry*, **46**, 8850–8860.
29. Gudasheva, T. A., Voronina, T. A., Ostrovskaya, R. U., Rozantsev, G. G., Vasilevich, N. I., Trofimov, S. S. *et al.* (1996). Synthesis and antiamnestic activity of a series of *N*-acylprolyl-containing dipeptides. *Eur. J. Med Chem.* **31**, 151–157.
30. Pelsman, A., Hoyo-Vadillo, C., Gudasheva, T. A., Seredenin, S. B., Ostrovskaya, R. U. & Busciglio, J. (2003). GVS-111 prevents oxidative damage and apoptosis in normal and Down's syndrome human cortical neurons. *Int. J. Dev. Neurosci.* **21**, 117–124.
31. Bukanova, J. V., Solntseva, E. I. & Skrebitsky, V. G. (2002). Selective suppression of the slow-inactivating potassium currents by nootropics in molluscan neurons. *Int. J. Neuropsychopharmacol.* **5**, 229–237.
32. Ostrovskaya, R. U., Gruden, M. A., Bobkova, N. A., Sewell, R. D., Gudasheva, T. A., Samokhin, A. N. *et al.* (2007). The nootropic and neuroprotective proline-containing dipeptide noopept restores spatial memory and increases immunoreactivity to amyloid in an Alzheimer's disease model. *J. Psychopharmacol.* **21**, 611–619.
33. Ostrovskaia, R. U., Gudasheva, T. A., Voronina, T. A. & Seredenin, S. B. (2002). [The original novel nootropic and neuroprotective agent noopept]. *Eksp. Klin. Farmakol.* **65**, 66–72.
34. Vorobyov, V., Kaptsov, V., Kovalev, G. & Sengpiel, F. (2011). Effects of nootropics on the EEG in conscious rats and their modification by glutamatergic inhibitors. *Brain Res. Bull.* **85**, 123–132.
35. Avedisova, A. S. & Yastrebov, D. B. (2007). Comparative efficiency of noopept and piracetam in therapy of astenic disorder of organic genesis. *Neurology*, **15**, 435–438.
36. Malisauskas, M., Ostman, J., Darinskas, A., Zamotin, V., Liutkevicius, E., Lundgren, E. & Morozova-Roche, L. A. (2005). Does the cytotoxic effect of transient amyloid oligomers from common equine lysozyme in vitro imply innate amyloid toxicity. *J. Biol. Chem.* **280**, 6269–6275.
37. Zamotin, V., Gharibyan, A., Gibanova, N. V., Lavrikova, M. A., Dolgikh, D. A., Kirpichnikov, M. P. *et al.* (2006). Cytotoxicity of albebetin oligomers depends on cross-beta-sheet formation. *FEBS Lett.* **580**, 2451–2457.

38. Winblad, B. (2005). Piracetam: a review of pharmacological properties and clinical uses. *CNS Drug Rev.* **11**, 169–182.
39. Neznamov, G. G. & Teleshova, E. S. (2009). Comparative studies of Noopept and piracetam in the treatment of patients with mild cognitive disorders in organic brain diseases of vascular and traumatic origin. *Neurosci. Behav. Physiol.* **39**, 311–321.
40. Gudasheva, T. A., Konstantinopol'skii, M. A., Ostrovskaya, R. U. & Seredenin, S. B. (2001). Anxiolytic activity of endogenous nootropic dipeptide cycloprolylglycine in elevated plus-maze test. *Bull. Exp. Biol. Med.* **131**, 464–466.
41. Kondratenko, R. V., Derevyagin, V. I. & Skrebitsky, V. G. (2010). Novel nootropic dipeptide Noopept increases inhibitory synaptic transmission in CA1 pyramidal cells. *Neurosci. Lett.* **476**, 70–73.
42. Ostrovskaia, R. U., Vakhitova Iu, V., Salimgareeva, M., Iamidanov, R. S., Sadovnikov, S. V., Kapitsa, I. G. & Seredenin, S. B. (2010). [On the mechanism of noopept action: decrease in activity of stress-induced kinases and increase in expression of neutrophines]. *Eksp. Klin. Farmakol.* **73**, 2–5.
43. Ehrnhoefer, D. E., Bieschke, J., Boeddrich, A., Herbst, M., Masino, L., Lurz, R. *et al.* (2008). EGCG redirects amyloidogenic polypeptides into unstructured, off-pathway oligomers. *Nat. Struct. Mol. Biol.* **15**, 558–566.
44. Gazit, E. (2002). A possible role for pi-stacking in the self-assembly of amyloid fibrils. *FASEB J.* **16**, 77–83.
45. Azriel, R. & Gazit, E. (2001). Analysis of the minimal amyloid-forming fragment of the islet amyloid polypeptide. An experimental support for the key role of the phenylalanine residue in amyloid formation. *J. Biol. Chem.* **276**, 34156–34161.
46. Gharibyan, A. L., Zamotin, V., Yanamandra, K., Moskaleva, O. S., Margulis, B. A., Kostanyan, I. A. & Morozova-Roche, L. A. (2007). Lysozyme amyloid oligomers and fibrils induce cellular death via different apoptotic/necrotic pathways. *J. Mol. Biol.* **365**, 1337–1349.
47. Xue, W. F., Hellewell, A. L., Hewitt, E. W. & Radford, S. E. (2010). Fibril fragmentation in amyloid assembly and cytotoxicity: when size matters. *Prion*, **4**, 20–25.
48. Seredenin, S. B., Voronina, T. A., Gudasheva, T. A., Ostrovskaya, R. U., Rozantsev, G. G., Skoldinov, A. P. *et al.* (1995). Biologically active *N*-acylprolyldipeptides having antiamnestic, antihypoxic effects. US Patent No. 5,439,930.
49. Delaglio, F., Grzesiek, S., Vuister, G. W., Zhu, G., Pfeifer, J. & Bax, A. (1995). NMRPipe: a multidimensional spectral processing system based on UNIX pipes. *J. Biomol. NMR*, **6**, 277–293.
50. Johnson, B. A. & Blevins, R. A. (1994). NMRView: a computer program for the visualization and analysis of NMR data. *J. Biomol. NMR*, **4**, 603–614.
51. Eliezer, D., Kutluay, E., Bussell, R., Jr. & Browne, G. (2001). Conformational properties of alpha-synuclein in its free and lipid-associated states. *J. Mol. Biol.* **307**, 1061–1073.
52. Rao, J. N., Kim, Y. E., Park, L. S. & Ulmer, T. S. (2009). Effect of pseudorepeat rearrangement on alpha-synuclein misfolding, vesicle binding, and micelle binding. *J. Mol. Biol.* **390**, 516–529.
53. Molina-Jimenez, M. F., Sanchez-Reus, M. I., Andres, D., Cascales, M. & Benedi, J. (2004). Neuroprotective effect of fraxetin and myricetin against rotenone-induced apoptosis in neuroblastoma cells. *Brain Res.* **1009**, 9–16.